

Supporting Information for

Boosting Sodium Storage of Fe_{1-x}S/MoS₂ Composite via Heterointerface Engineering

Song Chen^{1,2}, Shaozhan Huang², Junping Hu², Shuang Fan^{1,2}, Yang Shang², Mei Er Pam², Xiaoxia Li², Ye Wang⁴, Tingting Xu⁴, Yumeng Shi^{1,3,*}, Hui Ying Yang^{2,*}

¹International Collaborative Laboratory of 2D Materials for Optoelectronics Science and Technology of Ministry of Education, College of Optoelectronic Engineering, Shenzhen University, Shenzhen 518060, People's Republic of China

²Pillar of Engineering Product Development, Singapore University of Technology and Design, 8 Somapah Road, 487372, Singapore

³Engineering Technology Research Center for 2D Material Information Function Devices and Systems of Guangdong Province, College of Optoelectronic Engineering, Shenzhen University, Shenzhen 518060, People's Republic of China

⁴Key Laboratory of Material Physics of Ministry of Education, School of Physics and Engineering, Zhengzhou University, Zhengzhou 450052, People's Republic of China

*Corresponding authors. E-mail: yanghuiying@sutd.edu.sg (Hui Ying Yang); yumeng_shi@163.com (Yumeng Shi)

Supplementary Figures

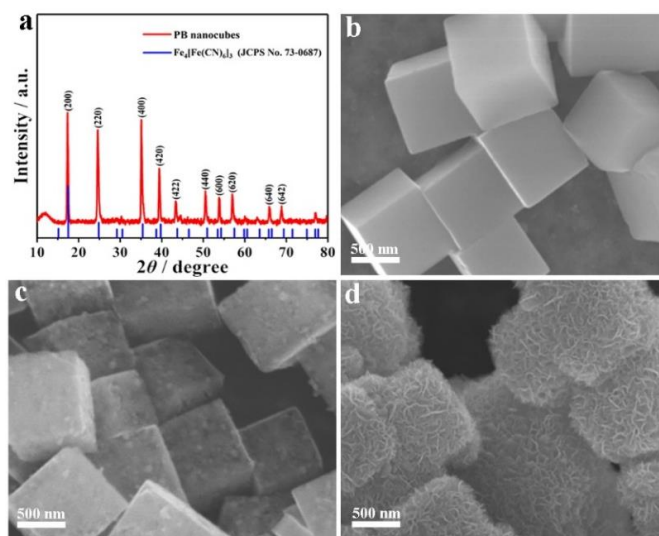


Fig. S1 a XRD pattern and b SEM image of PB nanocubes. SEM images of c FeCN nanocubes and d FeCN/MoS₂ composite

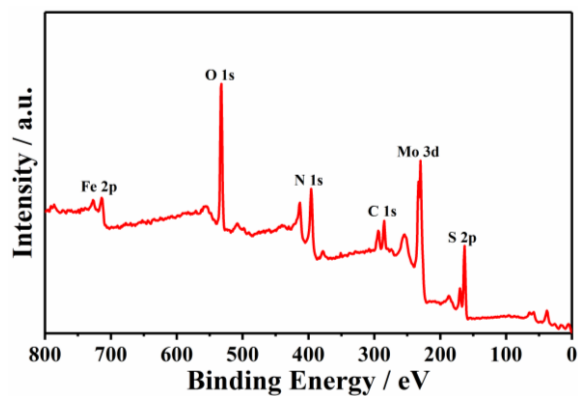


Fig. S2 Survey XPS spectra of the $\text{Fe}_{1-x}\text{S}/\text{MoS}_2$ composite

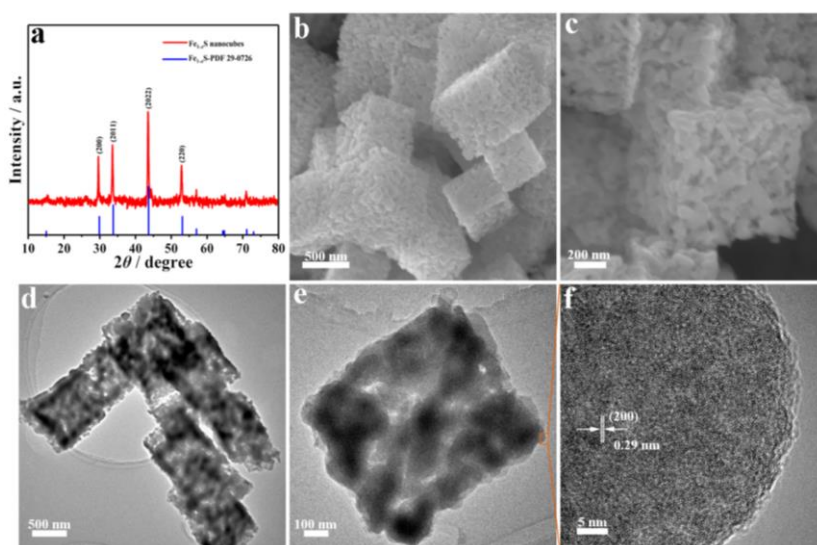


Fig. S3 **a** XRD pattern, **b**, **c** SEM images, **d**, **e** TEM images and **f** HRTEM image of Fe_{1-x}S nanocubes

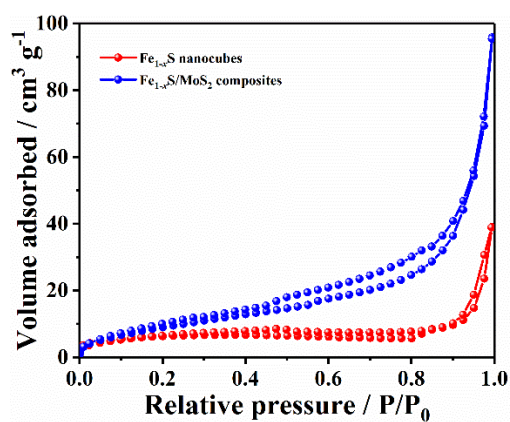


Fig. S4 Nitrogen adsorption-desorption isotherms of $\text{Fe}_{1-x}\text{S}/\text{MoS}_2$ composite/ Fe_{1-x}S nanocubes

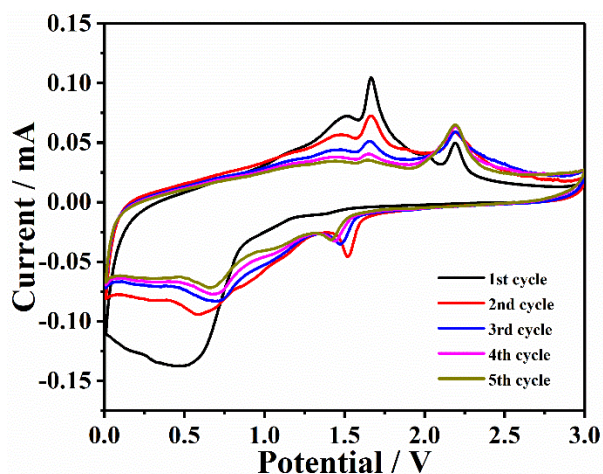


Fig. S5 CV curves of Fe_{1-x}S nanocube electrode for the first five cycles

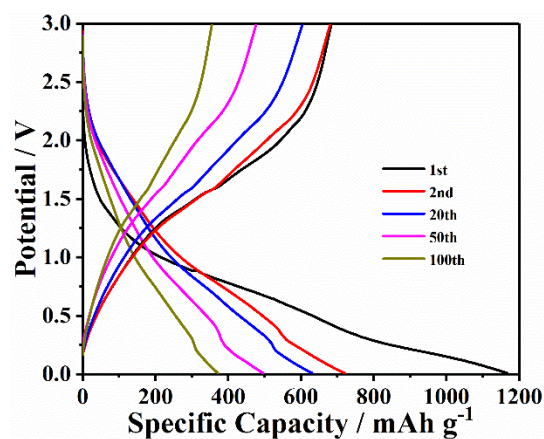


Fig. S6 Galvanostatic charge-discharge profiles of Fe_{1-x}S nanocube electrode at 100 mA g⁻¹

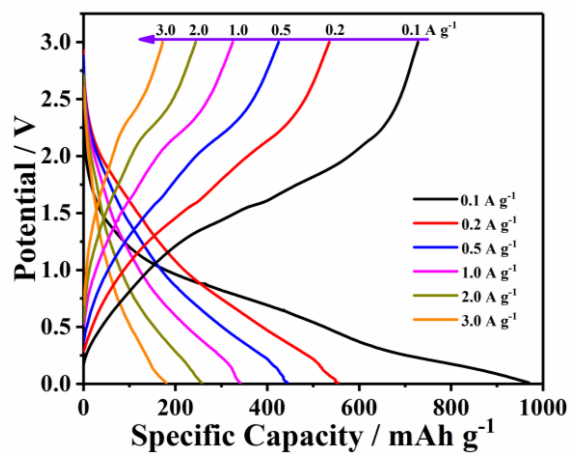


Fig. S7 Galvanostatic charge-discharge profiles of Fe_{1-x}S nanocube electrode at various current densities

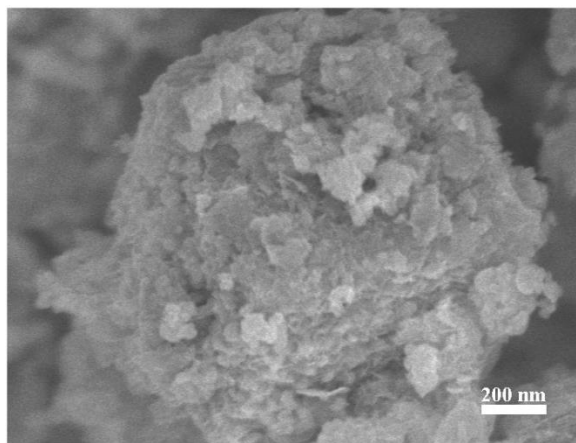


Fig. S8 SEM image of $\text{Fe}_{1-x}\text{S}/\text{MoS}_2$ composite after cycling

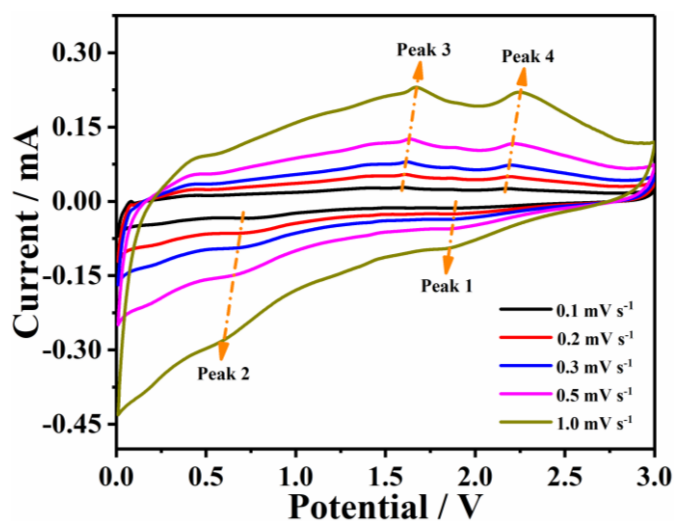


Fig. S9 CV curves of $\text{Fe}_{1-x}\text{S}/\text{MoS}_2$ composite at different scan rates

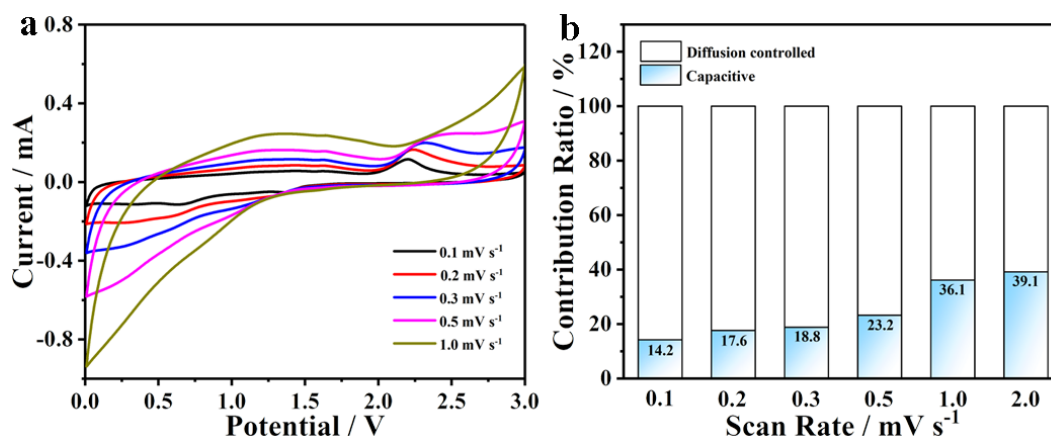


Fig. S10 **a** CV curves of Fe_{1-x}S nanocubes at different scan rates. **b** Normalized contribution ratio of capacitive capacities at different scan rates

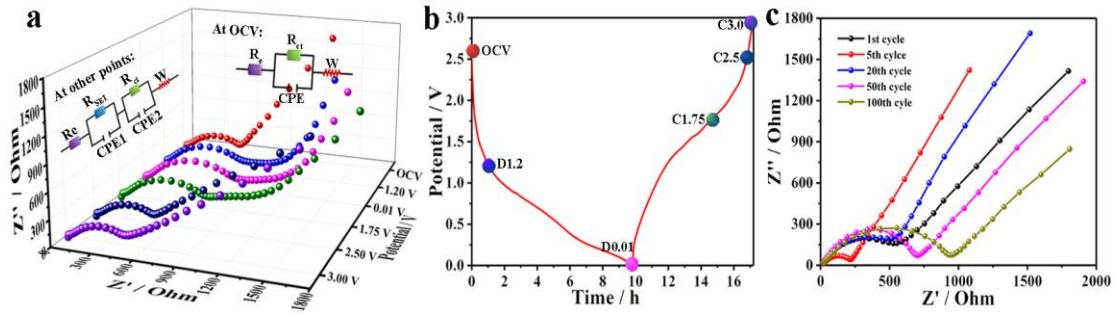


Fig. S11 **a** *In situ* EIS spectra evolution of Fe_{1-x}S electrode at different charge/discharge potentials. **b** First charge/discharge profile of Fe_{1-x}S electrode at 100 mA g^{-1} with labeled points for EIS. **c** EIS spectra of Fe_{1-x}S electrode after different cycles

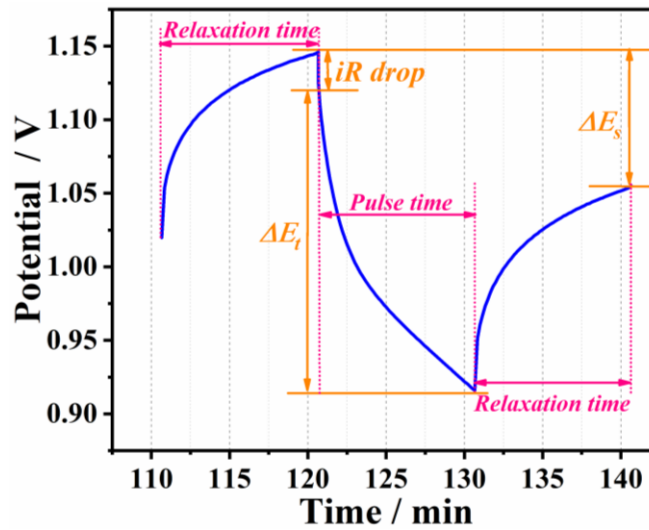


Fig. S12 E vs. t curve for a single GITT during discharge process

Na-ion chemical diffusion coefficient (D_{Na}) is calculated based on the following equation [S1]:

$$D = \frac{4L^2}{\pi\tau} \left(\frac{\Delta E_s}{\Delta E_t} \right)^2$$

where L is Na^+ diffusion length (approximately equal to the electrode thickness for compact electrode), τ is the relaxation time, ΔE_s is the steady state voltage change by the current pulse, ΔE_t is the voltage change during the current pulse after excluding iR drop.

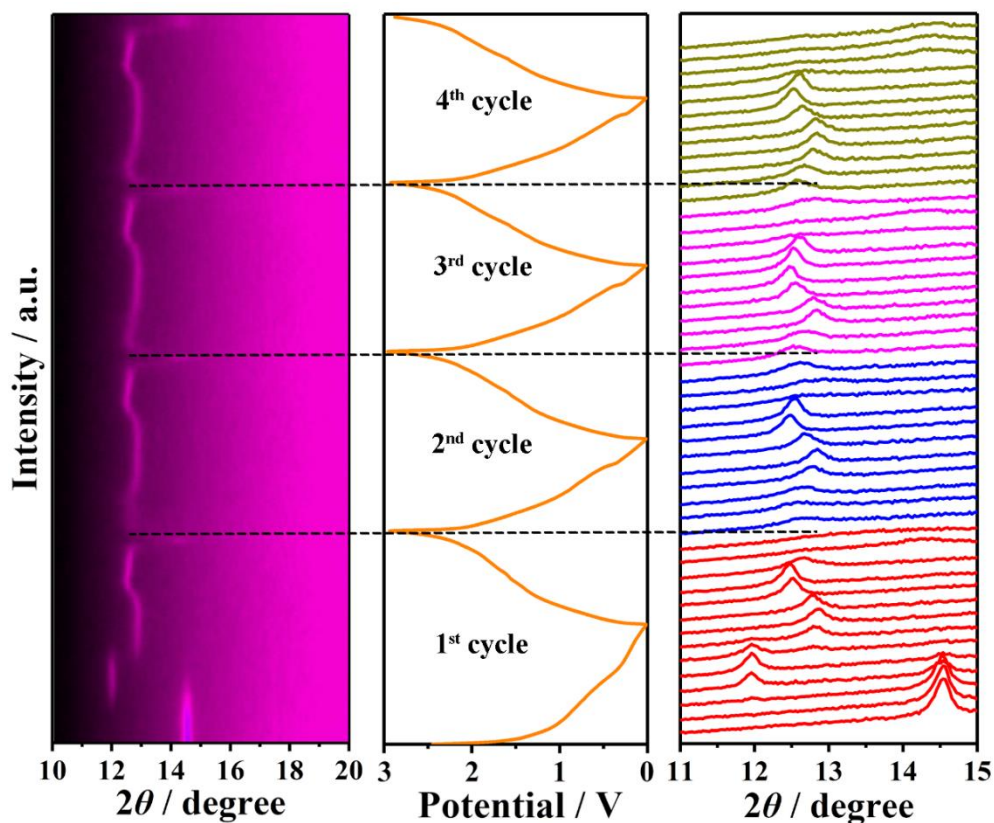


Fig. S13 Contour plots of *in situ* XRD results and the corresponding selected diffraction patterns of $\text{Fe}_{1-x}\text{S}/\text{MoS}_2$ composite electrode during the initial four cycles at 200 mA g^{-1}

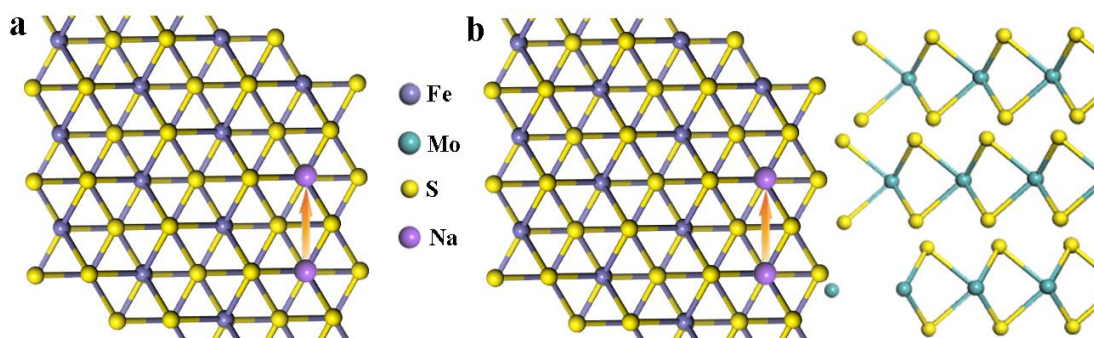


Fig. S14 The migration path on **a** Fe_{1-x}S surface, and **b** $\text{Fe}_{1-x}\text{S}/\text{MoS}_2$ interface

Supplementary References

[S1] D.T. Ngo, H.T.T. Le, C. Kim, J.Y. Lee, J.G. Fisher, I.D. Kim, C.J. Park, Mass-scalable synthesis of 3D porous germanium–carbon composite particles as an ultra-high rate anode for lithium ion batteries. *Energy Environ. Sci.* **8**, 3577-3588 (2015).

<https://doi.org/10.1039/C5EE02183A>